PAPER

Theoretical Proposal of an Optical Detection System Using DFB Laser with a Very Small Aperture

Minoru YAMADA[†a)], ***Regular Member***, **Daisuke KAWASAKI**[†], **Hirofumi AWABAYASHI**[†], ***Nonmembers***, ***and*** **Moustafa AHMED**[†], ***Regular Member***

SUMMARY An optical detection system using a DFB laser with a very small aperture is theoretically proposed. The threshold gain level in DFB laser is sensitively varied with combined reflections by the facet and the corrugation as well as with the optical injection reflected at the surface of the optical disk. Variation of the threshold gain level is counted as the voltage change on electrodes of the laser. It is found that sensitivity of the optical detection with a well-designed DFB laser becomes six times larger than that with conventional Fabry-Perot ones. Field distribution around the small aperture is analyzed taking into account both the near-field and the radiation field. Numerical data on the voltage change are given as examples of the detection system.

key words: *DFB laser, near field optics, very small aperture, optical pick-up, optical head*

1. Introduction

Recording technology with much high density in the optical disk is demanded toward increasing of information data. The recording density is restricted with the wavelength of the detecting light called as the diffraction limit. One possible idea to increase the density beyond the diffraction limit is to utilize the so called near-field component [1], [2]. The near-filed component can exude from a small aperture whose diameter is smaller than the half wavelength of the light.

Additional technology to support this idea is to make role the optical emitter as an optical detector. Insertion of a beam splitter as in the conventional optical pick-up prevents to approach both the emitter and the detector to the optical disk closely. Furthermore, power of the detecting light is weaker than 1/4 of the emitted light when a beam splitter with 50% transmittance is inserted.

Detection of the feedbacked light through variation of the electrode voltage on semiconductor lasers was firstly proposed by Mitsuhashi et al. [3], and was followed by Partovi to the case of a small aperture to utilize the near-field component [4].

The subjects toward realization of the above mentioned novel optical pick-up are to increase sensitivity of the detection and to make free from the feedback noise. Sensitivity of the detection should be reduced with reduction of the aperture size even if the near-field component is taken into account. Furthermore, semiconductor lasers tend to reveal excess noise called feedback noise when the output light is re-injected into the laser due to reflection at surface of the optical disk [5].

In this paper, we propose an optical detection system using a DFB (distributed feedback) laser with a very small aperture as shown in Fig. 1. Sensitivity of the detection can be increased due to combined effect of the corrugated and facet reflectors. Since the lasing longitudinal mode is uniquely selected by the DFB structure (corrugated reflector), the mode hopping or the mode competition phenomena among lasing modes are suppressed. The external cavity mode, which is formed by the laser facet and the optical disk, should not be built up because the distance between the laser facet and the optical disk is shorter than the optical wavelength. Then any phenomenon of mode competition will not be generated in the proposed device resulting in operation free from the feedback noise [6].

In Sect. 2, mechanisms of the proposed optical detection system are explained. In Sect. 3, the lasing condition is examined by extending the coupled mode theory of DFB laser [7], [8] to the case under optical reinjection [9]. In Sect. 4, properties of the optical field emitted from a circular aperture are analyzed based on a model supposing the electric and magnetic current sources. Contributions of the radiation and the near-

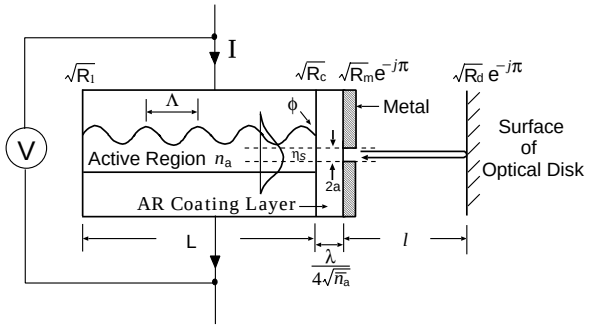

Fig. 1 Schematic illustration of the proposed optical detection system using a DFB laser with a very small aperture. Emitted light is reflected at surface of the optical disk and re-injected into the laser. The re-injected light is detected through change of the electrode voltages V on the laser.

Manuscript received July 11, 2001.
Manuscript revised October 12, 2001.

[†]The authors are with the Faculty of Engineering, Kanazawa University, Kanazawa-shi, 920-8667 Japan.
a) E-mail: myamada@t.kanazawa-u.ac.jp

field components are examined. In Sect. 5, changes of the electrode voltage with the optical re-injection are numerically evaluated through the equation of the lasing gain, which is originally formulated with the density matrix analysis [10], [11]. In Sect. 6, overall sensitivity of the proposed detection system is discussed.

2. Proposed System and Model of Analysis

The proposed device and detection system are schematically illustrated in Fig. 1. The basis of the device is a DFB semiconductor laser made of AlGaAs/GaAs crystals with cavity length L of several hundreds μm. The front facet of the laser is coated by AR (anti-reflection) and metal layers. A small hole with diameter $2a$ is prepared on the metal coating layer as an emitting aperture. The laser is in operation with injection current I. Reflected light from the surface of an optical disk re-injects into the laser. The electrode voltage V varies with the amount of the re-injected light.

Change of the electrode voltage originates from variation of the quasi-Fermi-levels of the electron and the hole in the active region. The quasi-Fermi-levels are almost clamped at values at the lasing threshold. The larger variation of the threshold carrier density with the optical injection gives the higher sensitivity in the detector.

The threshold gain level in a DFB laser sensitively changes with the spatial phase relation ϕ of the corrugated structure to the end facet [8]. We utilize this character to increase the detection sensitivity.

The AR layer is designed to achieve no reflection for the transmitting component from the semiconductor crystal to the free space. Thickness of the layer is then $\lambda/4\sqrt{\bar{n}_a}$, where λ is wavelength of the lasing field and $\bar{n}_a$ is the averaged refractive index in the active region. Therefore the boundary between the semiconductor crystal and the AR layer gives reflection in regions covered with the metal. The power reflectivities between semiconductor and the AR layer and the AR layer to the metal are put R_c and R_m, respectively, where

$$R_c = \left(\frac{\bar{n}_a - \sqrt{\bar{n}_a}}{\bar{n}_a + \sqrt{\bar{n}_a}} \right)^2 . \tag{1}$$

The power reflectivity at the back facet is R_1.

A simplified model to introduce the optical injection is shown in Fig. 2. The electric reflectivities at the back and the front facets are put as r_1 and r_2, respectively. r_1 is simply given as

$$r_1 = \sqrt{R_1} . \tag{2}$$

On the other hand, r_2 is characterized not only with R_c and R_m but also the optical emission from the emitting aperture. We assume the ratio of the transverse field distribution on the aperture of the guided mode to be η_s. Then we get

$$r_2 = \sqrt{1-\eta_s}\, \frac{\sqrt{R_c} + \sqrt{R_m}}{1 + \sqrt{R_c R_m}} \tag{3}$$

The optical injection is superposed on this r_2. An equivalent reflectivity r_2' is thus defined as

$$r_2' = r_2 + \sqrt{\Gamma_{total}}\, e^{-j\theta} \tag{4}$$

where Γ_{total} is an overall power re-injection ratio including the reflectivity at the surface of the optical disk and the coupling coefficient into the laser such as η_s, and θ is the phase delay.

The corrugated structure is represented as variation of the refractive index $n_a(z)$ in the active region,

$$n_a(z) = \bar{n}_a + \Delta n_a \cos(2\beta_B z + \phi) \tag{5}$$

where Δn_a is the amplitude of the variation, $2\beta_B = 2\pi/\Lambda$ is the spatial wavenumber and ϕ is the initial phase at $z = 0$ which is the front facet of the semiconductor crystal.

The sensitivity of the optical detection changes with the initial phase ϕ. Two representative structures are illustrated in Fig. 3. Models DFB(1) and DFB(2) are cases with $\phi = 1.5\pi$ and $\phi = 0.5\pi$, respectively.

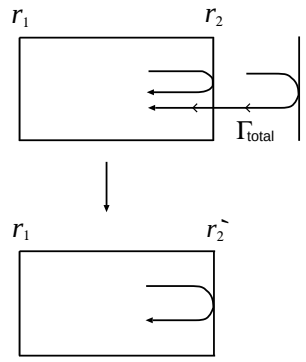

Fig. 2 A method taking the optical re-injection into account in terms of equivalent reflectivity r_2'.

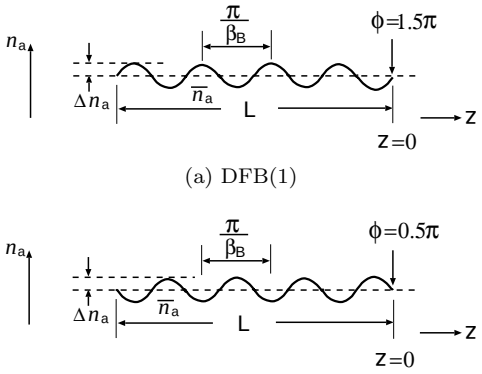

(a) DFB(1)

(b) DFB(2)

Fig. 3 Corrugation structures of DFB laser. Sensitivity of the detection varies with the initial phase ϕ. (a) Model DFB(1) has $\phi = 1.5\pi$. (b) Model DFB(2) has $\phi = 0.5\pi$.

3. Oscillating Condition

The oscillating condition of a DFB laser having facet mirrors is given as solutions of the following equation [9]

$$(1 - r_1 r_2' e^{-2j\beta_B L})\gamma \cosh(\gamma L) - \left\{ \left(\frac{g_{th} - \alpha_{loss}}{2} - j\Delta\beta \right) (1 + r_1 r_2' e^{-2j\beta_B L}) - j\kappa(r_2' e^{-j\phi} - r_1 e^{-2j\beta_B L + j\phi}) \right\} \sinh(\gamma L) = 0 \quad (6)$$

with

$$\gamma^2 = \left(\frac{g_{th} - \alpha_{loss}}{2} - j\Delta\beta \right)^2 + \kappa^2 \quad (7)$$

where g_{th} and α_{loss} are the threshold gain level and the loss coefficient, respectively. $\Delta\beta$ is difference between the wavenumber β of the lasing field and the spatial wavenumber β_B of the corrugation and is defined as

$$\Delta\beta = \beta - \beta_B \ . \quad (8)$$

κ is the coupling coefficient between the forward and the backward propagating waves due to the corrugation and is defined as

$$\kappa = \frac{\beta\, \Delta n_a}{2\, \bar{n}_a} \ . \quad (9)$$

Since Eq. (6) is an equation with complex numbers, values of both $g_{th} - \alpha_{loss}$ and $\Delta\beta$ are evaluated simultaneously as solutions of that equation. The oscillating condition of a Fabry-Perot laser is also determined by putting $\kappa = 0$ in Eqs. (6) and (7).

Numerical examples of the threshold gain level and the wavenumber are shown in Fig. 4, where the coupling coefficient, the threshold gain level and the wavenumber are given as normalized values to the cavity length L. The optical re-injection is not counted in this figure.

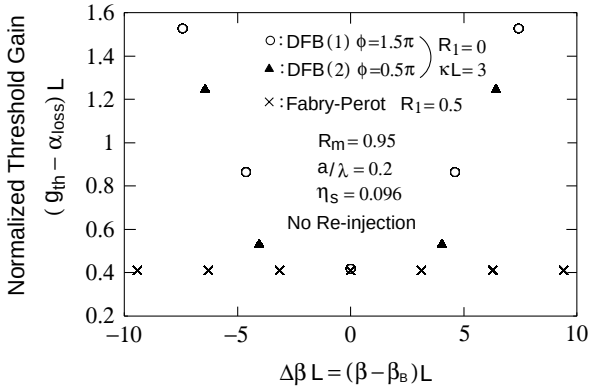

Fig. 4 Variation of the threshold gain level with wavenumber. The threshold gain levels for DFB(1), DFB(2) and Fabry-Perot laser marked with ◯, ▲, and ×, respectively.

As numerical parameters, $\bar{n}_a = 3.5$, $R_m = 0.95$ and $\eta_s = 0.096$ are assumed. In case of DFB lasers, $\kappa L = 3$ and $R_1 = 0$ are assumed. Condition of $R_1 = 0$ is suitable to optimize the detecting sensitivity. On the other hand, $R_1 = 0.5$ is assumed for the Fabry-Perot laser to get almost same threshold gain level with the DFB lasers.

The model DFB(1) gives the minimum threshold gain level at the Bragg wavelength, $\lambda = \Lambda/2$, or $\beta = \beta_B$. The model DFB(2) reveals the stop band at the Bragg wavelength and two minimum points of the threshold gain level slightly separated from the Bragg wavelength to the longer and the shorter wavelength sides. Results of the Fabry-Perot laser are also plotted in the figure.

4. Field Emission and Re-Injection

4.1 Basic Equations

The emitted field from an aperture should include not only radiation component but also near-field component at a position close to the aperture. We also have to determine whether the near-field component can be reflected at the surface of the optical disk and excites the lasing mode when the field is re-injected through the aperture. We analyzed the field emission and the re-injection by help of the so called equivalent current sources. An electric current source **J** and a magnetic current source **M** are supposed at the boundary, $(\xi, \eta, 0)$, between regions (1) and (2), as illustrated in Fig. 5. Transmission of the field into region (2) is formulated as excitations by these current sources by supposing the full space immersed uniformly with material of (2) as in Fig. 5(c), while reflection of the field to material (1) is formulated in uniform material of (1) as in Fig. 5(b). The values of the electronic and the magnetic current sources are equated with the incident, the reflected and the transmitted components at the boundary.

By following the above mentioned procedure, we get the transmitted, E_{tx}, H_{ty}, and reflected, E_{rx}, H_{ry},

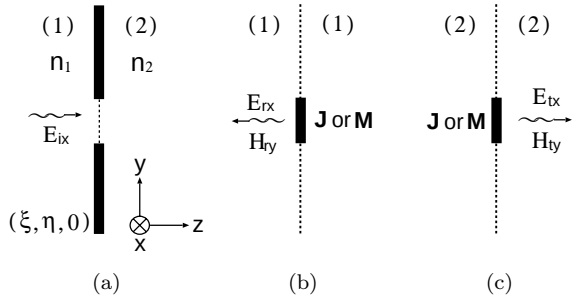

Fig. 5 Equivalent current sources at the boundary. An electric current source **J** and a magnetic current source **M** are supposed at the boundary between regions (1) and (2). (a) is the original structure. (b) is a model for field reflection into region (1). (c) is a model for field transmission into region (2).

components in integrated transformation forms from the incident electric field E_{ix} given as

$$E_{tx}(x,y,z) = \frac{2n_1}{n_1+n_2}\frac{1}{4\pi}\iint E_{ix}(\xi,\eta,0)\left\{jk_2 + \left(jk_2+\frac{1}{r}\right)\frac{z}{r}\right\}\frac{e^{-jk_2r}}{r}\,d\xi d\eta \quad (10)$$

$$H_{ty}(x,y,z) = n_2\sqrt{\frac{\epsilon_o}{\mu_o}}E_{tx}(x,y,z) \quad (11)$$

$$E_{rx}(x,y,z) = \frac{n_1-n_2}{n_1+n_2}\frac{1}{4\pi}\iint E_{ix}(\xi,\eta,0)\left\{jk_1 - \left(jk_1+\frac{1}{r}\right)\frac{z}{r}\right\}\frac{e^{-jk_1r}}{r}\,d\xi d\eta \quad (12)$$

$$H_{ry}(x,y,z) = -n_1\sqrt{\frac{\epsilon_o}{\mu_o}}E_{rx}(x,y,z) \quad (13)$$

with

$$k_1 = n_1\,\omega\sqrt{\mu_o\,\epsilon_o} \quad (14)$$

$$k_2 = n_2\,\omega\sqrt{\mu_o\,\epsilon_o} \quad (15)$$

$$r = \sqrt{(x-\xi)^2+(y-\eta)^2+z^2)} \quad (16)$$

Detailed processes to get these equations will be presented in somewhere by the authors.

In Eqs. (10) and (12), terms with jk are the radiation field components and those with $1/r$ are the near-field components. Conventional equations for field radiation are obtained by putting $z \approx r$ and by neglecting the term $1/r$ in these equations. Equations (10) and (12) tell us that the transmission and the reflection of the electric field are proportional to $2n_1/(n_1+n_2)$ and $(n_1-n_2)/(n_1+n_2)$, respectively, even when the near-field components are included. Also Eqs. (11) and (13) indicate that the magnetic field are combined to the electric field through the impedance $\sqrt{\mu_o/\epsilon_o}/n_2$ or $\sqrt{\mu_o/\epsilon_o}/n_1$ same as the case where only the radiation field is taken into account.

4.2 Field Emission

Optical emission from the small aperture with radius a is calculated with Eqs. (10) and (11) by supposing regions (1) and (2) to be the AR coating layer and the free space, respectively. The field distribution of $E_{ix}(\xi,\eta,0)$ is assumed uniform within the aperture. The metal of the coating is assumed to be an ideal material with $\sigma \to \infty$ and its thickness is zero for simple calculation. That is, absorption or scattering loss caused by wall of the metal when the field passes through the aperture is neglected here. Calculated data are shown in Fig. 6. Vertical axes are the normalized filed intensities

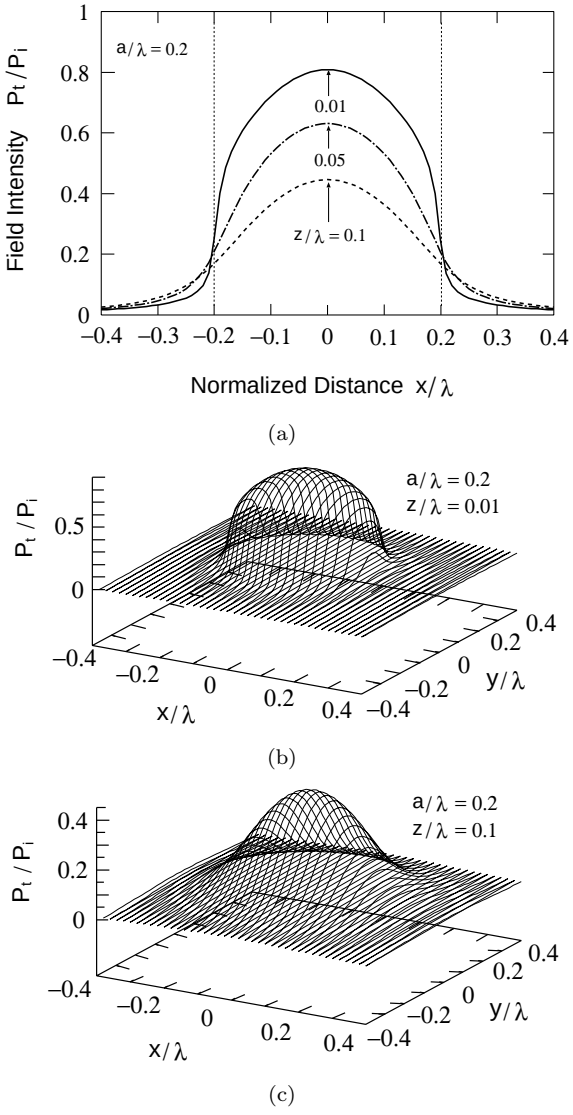

Fig. 6 Intensity profile of the emitted field. The field can be emitted even the aperture radius is much smaller than the wavelength.

$P_t/P_i = (n_2/n_1)\,|E_{tx}/E_{ix}|^2$. The distances are normalized with the wavelength λ. These figures are cases with $a/\lambda = 0.2$. The field can be emitted even if the aperture radius is much smaller than the wavelength.

Variations of the field intensity with distance z from the aperture along the longitudinal axis ($x = y = 0$) are shown in Fig. 7. Solid lines are the data including the radiation field and the near-field components. Dotted lines are those by counting only the radiation field component. The near-field exists at very close space to the aperture but rapidly decays when separating from the aperture.

4.3 Reflection at the Optical Disk

Several methods have been taken up as the recording

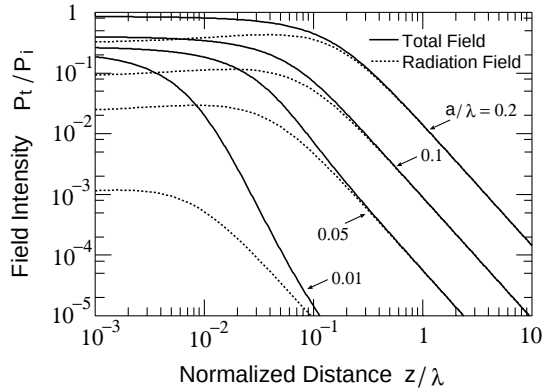

Fig. 7 Variations of the field intensity with distance z from the aperture along the longitudinal axis ($x = y = 0$). Solid lines are data including the radiation field and the near-field components. Dotted lines are those by counting only the radiation field component. The near-field exists at very close space to the aperture but rapidly decays when separating from the aperture.

mechanism on the optical disk. One is to change distance ℓ from the laser facet to the disk. Another metod is to change reflectivity of optical disk with change of the material property such as in chalcogenide amorphous semiconductors. However, the former method is not effective for application of the near-field, because neither the optical intensity nor the optical phase changes with variation of ℓ under condition of $\ell \ll \lambda$. Then the latter method may be the most feasible as the recording mechanism in our system.

Reflection at the surface of the optical disk could be calculated with Eqs. (12) and (13) by putting regions (1) and (2) as the free space and the material of the optical disk, respectively. However, we simply assume in this paper that power reflectivity at the optical disk is R_d and changes to $R_d(1-\Delta R_d)$ when data are recorded.

4.4 Re-Injection into Laser

Circular portion within radius a on the transverse distribution of the reflected light can enter the emitting aperture of the laser. Excitation of the lasing mode by the re-injected field is analyzed with Eq. (10) by putting regions (1) and (2) to be the free space and the AR coating layer, respectively.

We should summarize here structure of the total re-injection ratio Γ_{total} introduced in Eq. (4). The total re-injection ratio is expressed as

$$\Gamma_{total} = (\eta_s \eta_t)^2 \eta_w R_d \tag{17}$$

Here, η_s is the ratio of transverse field distribution on the aperture in the laser which was introduced in Sect. 2. η_t is the transmission efficiency passing through the aperture by suffering absorption or scattering loss from the metal wall. However, $\eta_t = 1$ is assumed in this paper with assumption of zero thickness of the metal coating for simple treatment. η_w is the ratio of field distribution on the area within radius a to the full distribution after propagation along $z = 2\ell$. R_d is the power reflectivity on the surface of the optical disk. Namely, the returning ratio of the emitted field into the aperture is counted as $\eta_w R_d$.

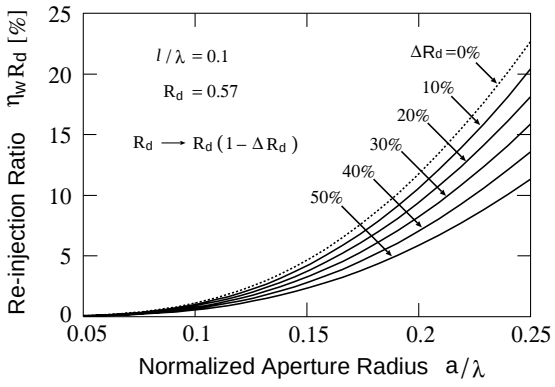

(a)

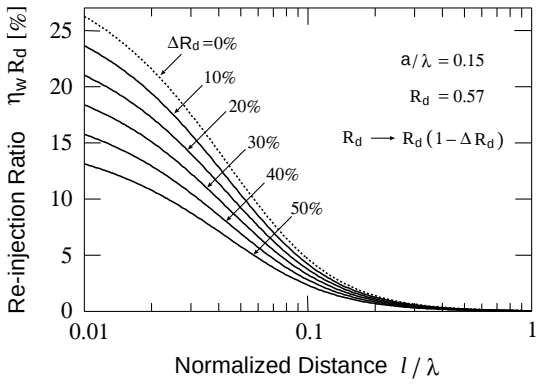

(b)

Fig. 8 The re-injection ratio. (a) is variation for the aperture radius. (b) is variation for the distance. The power reflectivity of $R_d = 0.57$ is assumed and the change of the reflectivity ΔR_d is given as a parameter.

Reading of the recorded data is done with change of the reflectivity from R_d to $R_d(1-\Delta R_d)$. Calculated examples of $\eta_w R_d$ are shown in Fig. 8. $R_d = 0.57$ is assumed with the refractive index of $n = 5.67 - 3.01j$ as a chalcogenide amorphous semiconductor. ΔR_d is given as a parameter.

5. Change of the Electrode Voltage

Re-injection of the reflected light changes the threshold gain level g_{th} as discussed in Sects. 2 and 3. The gain g_{th} is given as the product of the local gain g_{local} and the field confinement ratio ξ in the active region.

$$g_{th} = \xi \, g_{local} \tag{18}$$

The local gain g_{local} in semiconductor laser is characterized with the quasi-Fermi-levels μ_c in the conduction band and μ_v in the valence band. Difference of

these quasi-Fermi-levels is the electrode voltage V on the active region forming p-i-n junctions.

$$eV = (\mu_c - \mu_v) \tag{19}$$

The local gain is caused by electron transitions from the conduction band to the heavy hole and the light hole bands in the valence band and is given as

$$g_{local}(\hbar\omega) = \frac{\hbar\omega}{\tau_{in}\bar{n}_a}\sqrt{\frac{\mu_o}{\epsilon_o}}\sum_{j=h,l}\int_{W_g}^{\infty}|R_{cv}|^2 \times \frac{g_{cvj}(W)[f_{cj}(W) - f_{vj}(W)]}{(\hbar\omega - W)^2 + (\hbar/\tau_{in})^2}\,dW \tag{20}$$

where subscripts c and v indicate the conduction band and the valence band, respectively, j represents $j = h$ as the heavy hole band and $j = l$ as the light hole band. $\sum_{j=h,l}$ indicates to sum for the heavy and light hole bands. W is energy difference between an electron in the conduction band and a hole in the valence band, while W_g is the band gap energy given by

$$W_g = W_c - W_v \tag{21}$$

R_{cv} is the dipole-moment whose value is inversely proportional to W as [11]

$$|R_{cv}|^2 = \left(\frac{W_g}{W}\right)^2 |R_0|^2 \tag{22}$$

τ_{in} is the intra-band relaxation time [10]. The Fermi-Dirac functions and the density of the state are defined for the electron-hole pair (ambipolar or dipole) as,

$$f_{cj}(W) = \frac{1}{1 + \exp\left[\frac{\frac{m_j}{m_c+m_j}(W - W_g) - \mu_c + W_c}{kT}\right]} \tag{23}$$

$$f_{vj}(W) = \frac{1}{1 + \exp\left[\frac{-\frac{m_c}{m_c+m_j}(W - W_g) - \mu_j + W_v}{kT}\right]} \tag{24}$$

$$g_{cvj}(W) = \frac{1}{2\pi\hbar^3}\left(\frac{2m_c m_j}{m_c + m_j}\right)^{\frac{3}{2}}\sqrt{W - W_g} \tag{25}$$

where m_c and m_j are the effective masses of the electron and hole, respectively.

The Fermi-Dirac functions are characterized through either μ_c or μ_v not with V explicitly. Detailed values of μ_c and μ_v are determined to satisfy the following neutral condition in an intrinsic semiconductor material.

$$\int_{W_g}^{\infty}[\{f_{ch}(W,\mu_c) + f_{vh}(W,\mu_v) - 1\}g_{cvh}(W) + \{f_{vl}(W,\mu_v) - 1\}g_{cvl}(W)]\,dW = 0 \tag{26}$$

The variation of the local gain g_{local} with voltage V is calculated as follows : First, we set the electrode voltage V of Eq. (19). Second, we determine the quasi-Felmi-levels μ_c and μ_v to satisfy Eq. (26) by performing the numerical integration. Third, we calculate the local gain $g_{local}(\hbar\omega)$ by performing the numerical integration for various values of $\hbar\omega$ in Eq. (20). Finally, the peak value of g_{local} for variation of $\hbar\omega$ is determined. Thus, we obtain Fig. 9 as the characteristic relation between the local gain and the electrode voltage.

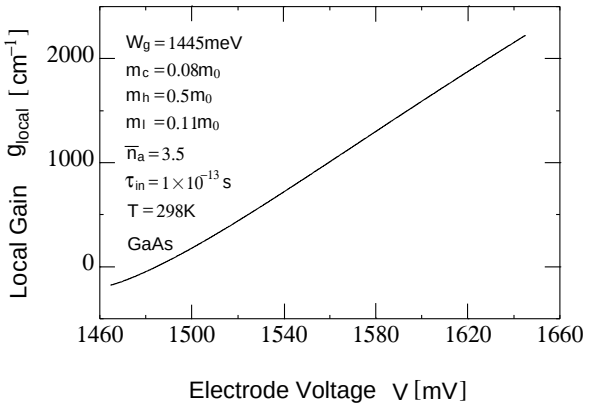

Fig. 9 Variation of the local gain with the electrode voltage in GaAs lasers.

A GaAs crystal is assumed as the active region with numerical parameters of $W_g = 1.445\,\mathrm{eV}$, $m_c = 0.08\,m_0$, $m_h = 0.5\,m_0$, $m_l = 0.11\,m_0$, $\bar{n}_a = 3.5$, $\tau_{in} = 1 \times 10^{-13}\,\mathrm{s}$, $|R_0|^2 = 2.77 \times 10^{-57}\mathrm{C}^2\mathrm{m}^2$ and $T = 298\,\mathrm{K}$.

6. Overall Sensitivity

The threshold gain level is reduced with the re-injection of the optical field. The voltage change ΔV is defined as the difference between the electrode voltage under the optical re-injection and that at no optical re-injection. This change does not relate directly to the value of the injection current I if the laser is in oscillation with condition of $I > I_{th}$. If ohmic loss for the current injection exists, the voltage change will be obstructed. We ignore the ohmic loss in this paper as an ideal case.

Dependencies of the voltage change on the re-injection ratio are shown in Fig. 10. The model of DFB(1) reveals the largest change of the electrode voltage. Dependencies on the initial phase ϕ of the corrugated structure are given in Fig. 11. As found in these figures, the voltage change becomes largest in the model of DFB(1), where the initial phase is $\phi = 1.5\pi$ and wavelength of lasing mode coincides with the Bragg wavelength that corresponds to the lowest threshold gain level. While the case of $\phi = 0.5\pi$ or 2.5π can not give sufficient voltage change represented as the model of DFB(2).

Both amplitude and phase relations between reflected component by the corrugated structure and that by the end facet critically affect the threshold gain level in the DFB laser. The re-injection of the optical field

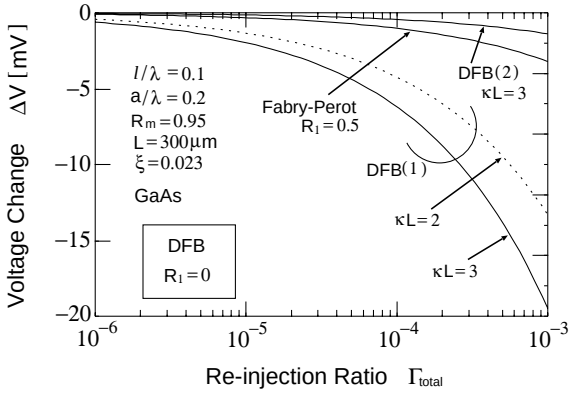

Fig. 10 Voltage change vs. Re-injection ratio. The voltage change becomes the largest of three-types lasers in the model of DFB(1).

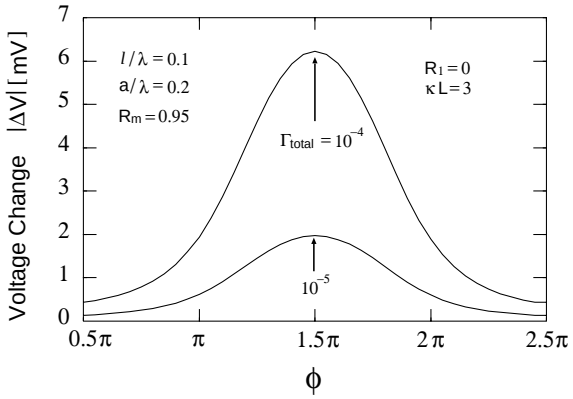

Fig. 11 Voltage change vs. Initial phase of the corrugation. The models DFB(1) and DFB(2) are $\phi = 1.5\pi$ and $\phi = 0.5\pi$, respectively.

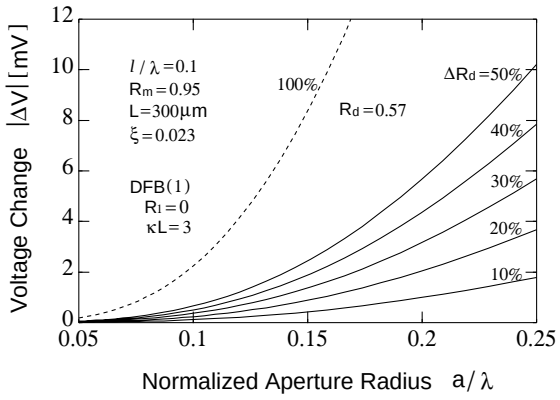

(a)

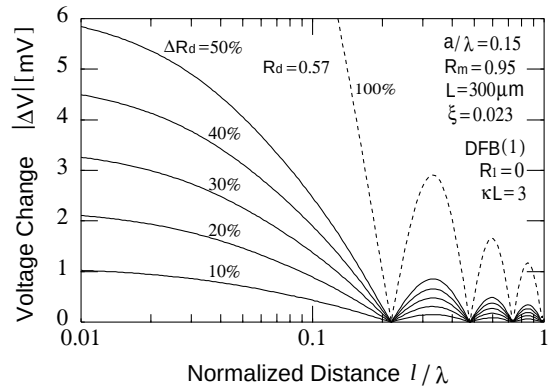

(b)

Fig. 12 Voltage change as function of the reflectivity change. (a) is dependence with the aperture radius. (b) is dependence with the distance to the optical disk.

works to change the effective reflectivity of the end facet as given by Eq. (4).

Then, variation of the threshold gain level on the effective reflectivity becomes more sensitive in the DFB laser than in the Fabry-Perot laser if the phase relation between reflection by the corrugation structure and the end facet is suitably set. The coupling coefficient κ becomes larger, the larger variation of the threshold gain level is obtained. Of course, accurate fabrication will be required to set the spatial initial phase ϕ exactly.

Dependencies of the voltage change on the aperture radius a and the distance ℓ to the optical disk are shown in Fig. 12. In this figure, the voltage change ΔV is defined as the voltage difference between operation with reflectivity R_d and that with $R_d(1 - \Delta R_d)$. The case $\Delta R_d = 100\%$ corresponds to the voltage change between operation under the re-injection with R_d and that without re-injection. Ranges $0 \leq \ell \leq \lambda/4$ and $\lambda/2 \leq \ell \leq 3\lambda/4$ have in-phase relation of the emitted field to the re-injected field. Ranges $\lambda/4 \leq \ell \leq \lambda/2$ and $3\lambda/4 \leq \ell \leq \lambda$ have a counter phase.

If we require 1mV of the voltage change as the optical detection, aperture radius of $a = 0.15\lambda$, distance of $\ell = 0.1\lambda$ and variation of reflectivity of $\Delta R_d = 20\%$ should be prepared.

7. Conclusions

An optical detection system using a DFB laser with a very small aperture is proposed and its operation is theoretically analyzed. The optical detection is done by detecting the change of the electrode voltage on the laser. The optical emission and re-injection through the very small aperture are analyzed. A DFB laser which oscillates with the Bragg wavelength gives sensitivity almost six times higher than the Fabry-Perot type laser.

Acknowledgement

This research is done under cooperation with TDK Corporation.

References

[1] E. Betzig, J.K. Trautman, R. Wolfe, E.M. Gyorgy, and P.L. Finn, "Near-field magneto-optics and high density data storage," Appl. Phys. Lett., vol.61, no.2, pp.142–144, 1992.
[2] S. Hosaka, T. Shintani, M. Miyamoto, A. Hirotsune, M. Terao, M. Yoshida, K. Fujita, and S. Kämmer, "Nanometer-sized phase-change recording using a scanning near-field optical microscope with a laser diode," Jpn. J. Appl. Phys.1, Regul. Pap. Short Notes, vol.35, no.1B, pp.443–447, 1996.
[3] Y. Mitsuhashi, J. Shimada, and S. Mitsutsuka, "Voltage change across the self-coupled semiconductor laser," IEEE J. Quantum Electron., vol.17, no.7, pp.1216–1225, 1981.
[4] A. Partovi, "Optical near-field aperture storage technique(ONFAST) for high density, high performance data storage applications," SPIE, vol.3864, pp.352–354, 1999.
[5] T. Morikawa, Y. Mitsuhashi, J. Shimada, and Y. Kojima, "Return-beam-induced oscillations in self-coupled semiconductor lasers," Electron. Lett., vol.12, pp.435–436, Aug. 1976.
[6] M. Yamada, "Theory of mode competition noise in semiconductor injection lasers," IEEE J. Quantum Electron., vol.QE-22, no.7, pp.1052–1059, 1986.
[7] H. Kogelnik and C.V. Shank, "Coupled-wave theory of distributed feedback lasers," J. Appl. Phys., vol.43, no.5, pp.2327–2335, May 1972.
[8] K. Kishino and S. Arai, "Lasing conditions of integrated lasers," in Handbook of Semiconductor Lasers and Photonic Integrated Circuits, eds. Y. Suematsu and A.R. Adams, pp.371–374, Chapman & Hall, London, 1994.
[9] M. Suhara and M. Yamada, "Analysis of excess intensity noise due to external optical feedback in DFB semiconductor lasers on the basis of mode competition theory," IEICE Trans. Electron., vol.E76-C, no.6, pp.1007–1017, June 1993.
[10] M. Yamada and Y. Suematsu, "Analysis of gain suppression in undoped injection lasers," J. Appl. Phys., vol.52, no.4, pp.2653–2664, April 1981.
[11] M. Asada, A. Kameyama, and Y. Suematsu, "Gain and intervalence band absorption in quantum-well lasers," IEEE J. Quantum Electron., vol.QE-2, no.7, pp.745–753, 1984.

Minoru Yamada was born in Yamanashi, Japan on January 26, 1949. He received the B.S. degree in electrical engineering from Kanazawa University, Kanazawa, Japan in 1971, and M.S. and Ph.D. degrees in electronics engineering from the Tokyo Institute of Technology, Tokyo, Japan in 1973 and 1976, respectively. He joined Kanazawa University in 1976, and is presently a Professor. From 1982 to 1983, he was a Visiting Scientist at Bell Laboratories, Holmdel, NJ, U.S.A. He is currently working in semiconductor injection laser, semiconductor modulator, and unidirectional optical amplifier. Dr. Yamada received the Yonezawa Memorial Prize in 1975, the Paper Award in 1976, and the Achievement Award in 1978 from the IEICE of Japan.

Daisuke Kawasaki was born in Niigata, Japan on June 22, 1975. He received the B.S. and M.S. degrees in electrical and computer engineering from Kanazawa University, Kanazawa, Japan in 1999 and 2001, respectively. He joined NEC Corporation in 2001.

Hirofumi Awabayashi was born in Toyama, Japan on September 24, 1977. He received the B.S. degree in electrical and computer engineering from Kanazawa University, Kanazawa, Japan in 2000. He is presently working toward the M.S. degree at Kanazawa University.

Moustafa Ahmed was born in El-Minia, Egypt on September 20, 1966. He received the B.Sc. and M.Sc. in Physics from Minia University, Egypt in 1988 and 1993, respectively. He received the Ph.D. degree in Electrical Engineering from Kanazawa University, Japan in 1999. In 1988 he was appointed as assistant lecturer at the Department of Physics, Minia University, Egypt, and since 2000 he has been working as a lecturer at the same department. From September 2000 to August 2002, he is a post-doctoral fellow at the Department of Electrical and Electronic Engineering, Kanazawa University, Japan. He is currently working in injection semiconductor lasers.